13^{th} European Conference on Mixing
London, 14-17 April 2009

ON THE RHEOLOGICAL BEHAVIOUR OF BATCH CRYSTALLISATIONS

Frans L. Muller

AstraZeneca, Hursfield industrial estate Macclesfield SK10 2NA UK
Frans.Muller@AstraZeneca.com

Abstract: During batch processing the formation of a solid phase is often accompanied by a significant reduction in the mobility of a reaction mass as a “soft” solid is formed. Often the fluid becomes stagnant with a mobile zone or “cavern” around the agitator. This phenomenon was investigated using two in-situ probes (i) a particle size probe which detected the onset of crystallisation and (ii) a viscosity probe which detected the onset and extent of rheological problems. The viscosity probe measurement appears to correlate with the yield-stress of the slurry. A mechanistic analysis of the phenomenon suggests a new dimensionless number: the Nienow number (Ni), the ratio of turbulent stresses to the yield stress of a fluid. Complete mobility is generally achieved for Ni > 30. These systems scale with tip speed if super-saturation is controlled.

Key words: Yield stress, Crystallising, in-situ viscometer probe, Cavern flow, Nienow number

1 INTRODUCTION

Rheological problems are frequently encountered in batch processes during which solids crystallise or precipitate from a solution. Typically a mobile system will suddenly “go thick” and then “on stirring” the fluid “thins out”. The rheology of these processes are difficult to assess, as they are extremely time and equipment dependent. For batch processes, a typical concentration of precipitated solids is about 1kg suspended in 4 to 10 L of an inviscid solvent; i.e. 5 – 20 vol% hold up. The slurry viscosity of inert particles may be described as function of solid content (Borghesani 1985, Gay et al. 1969, Heymann et al 2002):

$$\mu_{slurry} = \frac{\mu_{solvent}(T)}{\left(1-\left(\frac{\phi}{\phi_{crit}}\right)^{a}\right)^{b}} \qquad (1.)$$

Here μ represents the viscosity and ϕ the volume fraction of the solid phase. For instance using a=2 and b=1 was used to empirically describe concentrated slurries containing glass ballotini (Figure 1 shows that for (non crystallising) slurry systems no significant increase in viscosity is expected at solid concentrations below 20 vol%. Clearly when systems set “solid”

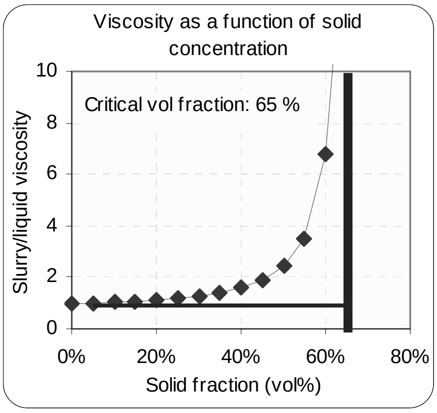

Figure 1: typical effect of solid concentration on viscosity

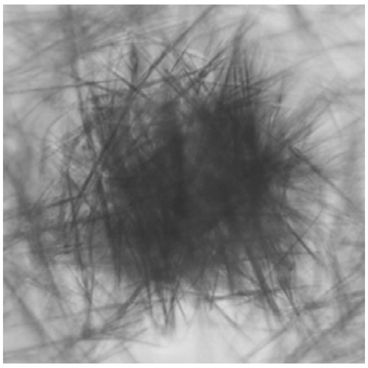

Figure 2: A tangle of crystals

the particles must interact in a way different to that described by equation 1. In this paper it is postulated that growing particles form a tangle of crystals (figure 2), and that the extent of tangling is a function of shear and time. A case study is presented which demonstrates this behaviour, and a qualitative model is presented to identify the main parameters that govern the rheology of crystallising processes.

2 CASE STUDY: THE CRYSTALLISATION OF CAFFEINE

Caffeine was chosen as the model system as it has properties similar to many compounds in industry: (i) it forms long thin needles (ii) its solubility is 20 mg/ml at 20 °C and doubles roughly every 20 °C and **unlike** most pharmaceutical intermediates, it is readily available and relatively harmless.…

2.1 Experimental

A 500mL jacketed glass reactor (ID 0.11 m) was equipped with a Mettler-Toledo FBRM Lasentec D600L probe and a Hydramotion RV900 viscosity probe. The reactor was agitated with a 4 blade pitch blade agitator (D/T=0.36, Z/T = 0.18) and temperature controlled by a programmable Huber Tango thermostatic bath

The D600L probe is well established in the crystallisation development community, and measures the chord lengths of particles in suspension. This author prefers to monitor the count of particles (#) multiplied by the mean chord length (μm) in order to observe an obscuration that is independent of the chord length but still highly non-linear with respect to particle concentration (very sensitive at low readings, not sensitive at high readings)

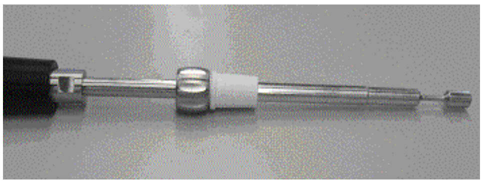
Figure 3: The hydramotion RV900 probe

The Hydramotion RV900 viscometer is a new instrument recently acquired (Figure 3). It is based on a resonant vibrational design in which the probe’s “bob” twists back and forth at very high frequency and shears through the surrounding fluid. Energy is lost due to viscous drag on the bob, and this loss can be correlated to the viscosity of the fluid. In non-Newtonian fluids this probe gives the apparent viscosity associated to very high shear rates. The shear rate is estimated at 5000 to 10000 s^{-1} based on work with power-law model liquids (not reported here).

The probe’s measurements (at 0.5 Hz) are independent of orientation in the vessel and proximity to walls, baffles and the agitator as the viscosity is measured from a layer close to the surface of the bob, typically a few tens of microns thick.

The experimental procedure is to charge 25 g (50 mg/mL, 5wt%) of caffeine (anhydrous and 500mL of deionised water were charged to the vessel (H/T = 0.68). The vessel was subsequently heated to 50°C dissolving the caffeine completely. The vessel was then cooled down to 37°C to supersaturate the solution. 0.25 g (0.5mg/mL, 0.05wt%) caffeine-hydrate seed (air dried product from a previous experiment; 100 μm long needles, 5μm wide) was added. The mass was held for 1 hr at 37°C then cooled to 20°C over 5 hour.

2.2 Results

Three experiments where conducted, (i) at a typical lab speed of 400 rpm (figure 4a), (ii) at a speed of 900 rpm (figure 4b), more representative of the plant (ND = 0.6 m/s, Re = 66000, P/V is estimated at ~800 W/m^3 using the power number representative of the plant vessel’ configuration). Finally (iii) was at 900 rpm but with double the amount of caffeine (higher temperatures were required to dissolve all material).

The data from the experiment at 400 rpm, displayed in figure 4a, clearly demonstrate a sequence that chemists (and associated engineers) often observe in the lab: (a) all seems to go well, no particles and no rheology problems, (b) the system goes cloudy but remains mobile (c) the system “sets solid” the mass now has a yield stress, and even though the agitator is turning, no fluid motion is observed at the wall of the vessel… a cavern has formed (Nienow

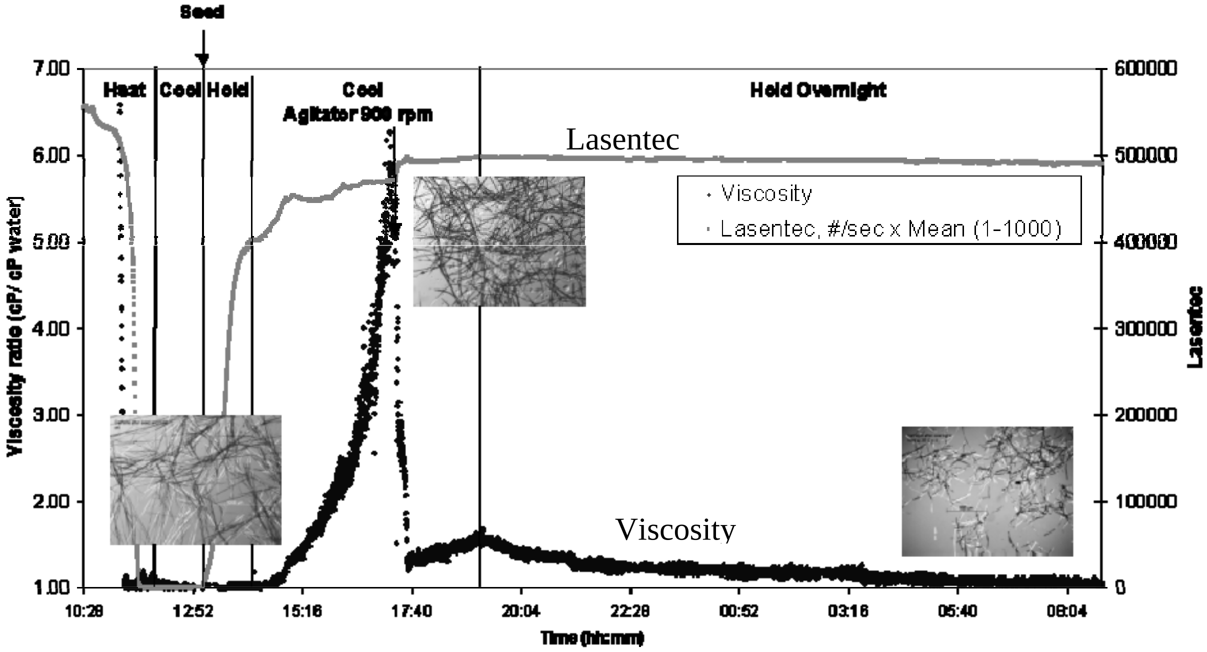

Figure 4a: Data for a caffeine crystallisation at **400 rpm**. Note the agitator speed had to be increased to 900 rpm to keep the system mobile.

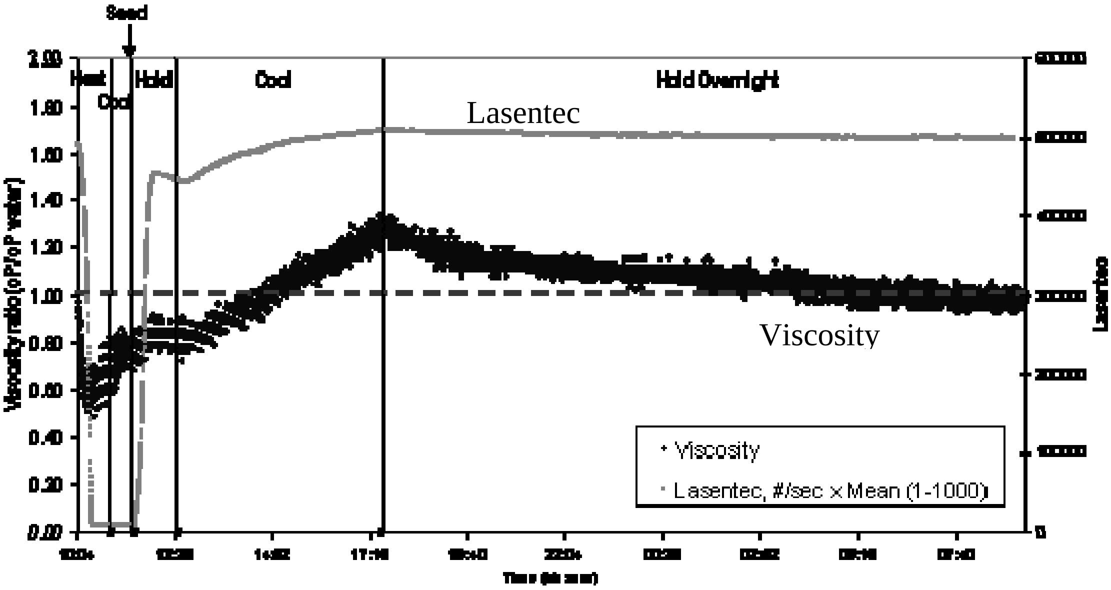

Figure 4b: Data for a caffeine crystallisation at **900 rpm**. Note the initial part of the viscosity curve is affected by the presence of a significant amount of bubbles, some attached to the probe

and Elson 1988) (d) the agitation rate is nervously increased, and … (e) release, the system remobilised. After leaving overnight (vi) the system is fully mobile and inviscid.

The second run at 900 rpm was a little frothy to start with, but once the crystallisation commenced also showed an increase in viscosity, although only little compared to the 400 rpm experiment. The final experiment, at double the caffeine strength has a trace similar to figure 4a, and the speed had to be increased from 900 rpm to 1200 rpm to keep this system mobilised. (peak viscosity was 15 cP)

2.3 Analysis

In all three experiments the particle obscuration as measured by the D600L probe increases rapidly after seeding to reach 80% to 90% of the final value after the 1 hour hold. The increase in obscuration is mainly due to the increase in length (i.e. the same particle is seen more frequently). The seed has lengthened in the order of 20 times (100 μm to 2 mm!). In this sense caffeine is an extreme case; a more typically the seed is smaller.

The microscope pictures of the solids formed at various time points in the experiment demonstrate that the caffeine indeed grows into very long needles during the hold. The viscosity probe does however not pick up significant structure until the mixture is cooled and the bulk of the solute crystallises out (note the last 20% rise in the signal of the D600L probe trace represents a the majority of solid formed).

The viscosity measured is relatively low throughout the crystallisation, less than 6 times the continuous phase viscosity. The system did actually set solid (no motion observed through the wall of the glass reactor) and the speed had to be increased to 900 rpm to remobilise. Clearly a structure had formed strong enough to resist the flow. When running the same experiment at 900 rpm throughout (figure 4b), viscosity also increases during the crystallisation, but to a much lesser extend. So structure is also being formed, but it is being broken up at a rate sufficiently high to prevent it from setting. Increasing the concentration to 10 wt% caffeine causes the formation of structure to accelerate to such an extent that structure can be formed that resists the flow up to 1200 rpm

In addition to the probe data, we also observed that the flow at the wall of the reactor stopped; this means the fluid has developed a yield stress and a cavern system has formed. This concept is illustrated in figure 5 where a cavern in a carbopol solution is visualised using a green food colouring dye.

Once the flow at the wall had stopped the agitation speed was increased just enough to remobilise the system. This new speed can be used to estimate the yield stress using the cavern calculation originally devised by Nienow and Elson (1988). They state that the torque on the agitator shaft is balanced against the moment generated by the yield stress on the cavern surface:

$$\begin{aligned}\text{Shaft Torque} &= \text{arm x force} \\ &\sim D_{cav} \text{ x } \text{Area}_{cav}\, \sigma_y \\ &\sim D_{cav}^2 H_{cav}\, \sigma_y\end{aligned} \qquad (2.)$$

where D_{cav} is the diameter of the cavern and σ_y the yield stress of the fluid. With the torque being equal to $P/2\pi N$ and assuming the height of the cavern is proportional to the cavern diameter we find that:

$$\left(\frac{D}{D_{cav}}\right)^3 \sim \sigma_y D^3 \frac{N}{P} \sim \frac{1}{Po} \frac{\sigma_y}{\rho N^2 D^2} \qquad (3.)$$

250 rpm **500 rpm** **700 rpm** .

Figure 5: Cavern Formation - 0.15 wt % Carbopol 980 in water (500 mL scale)

So by increasing the speed to grow the cavern size D_{cav} to T we can get an estimate of the yield stress by rearranging of equation (3):

$$\sigma_y \sim Po\,\rho N^2 D^2 \left(\frac{D}{T}\right)^3 \quad (4.)$$

Using P_o=1 (badly baffled PBT) the agitation speed required to just remobilise the slurry is sufficient to estimate the yield stress from equation (4). Interestingly, the estimate of the yield stress obtained correlates very well with the peak viscosity measured by the RV900 viscosity probe. The peak viscosity is measured just when the system becomes stagnant (figure 6). This is an observation important for the practical aspects of working with complex rheological systems; however no work was done to understand why the probe's measurements correlate with the yield stress.

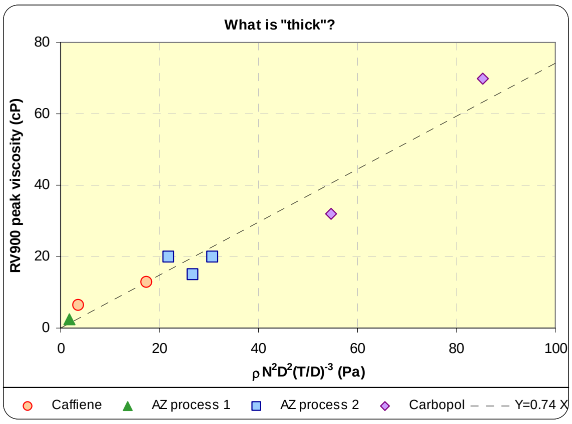

Figure 6: Peak viscosity measured versus the estimated yield stress for the caffeine system, but also for other experimental systems not reported here.

3 A SCALE UP MODEL FOR CRYSTALLISING RHEOLOGIES

In order to (a) develop processes that avoid setting, and (b) scale up processes that do have a tendency to set a model was constructed to identify the key scale up parameters.

3.1 Average centre point distance between particles

The first assumption of this model is that the particles have a high aspect ratio; they are rods or needles with a length l_p and width and depth assumed equal (d_p). Further it is taken that the particles are randomly distributed through the continuous phase. These assumptions typically hold for pharmaceutical systems in which needles are formed. For such systems, with a particle concentration C_p (number/m^3), the average centre to centre distance $\delta_{p\text{-}p} = 1/C_p^{1/3}$. For the particles to touch each other the aspect ratio $l_p/\delta_{p\text{-}p}$ must be larger than 1. It can easily be shown that this is the case if:

$$\frac{l_p}{d_p} \geq \sqrt{1/\varepsilon_p} \quad (5.)$$

here ε_p is the volume fraction of particles. Well-controlled crystallisations are typically seeded with up to 1% of the expected crystal mass, which would require an aspect ratio l_p/d_p >30 to form a network, but after 10% of the solute has crystallised this is reduced to an aspect ratio of 10, which is not uncommon. On completion of the crystallisation, the aspect ratio required is only ~4.

The growing rate of the seed particles is controlled with a temperature profile to ensure the crystals grow, rather than new crystals being formed due to nucleation. This means that no new particles are formed during the crystallisation. The seed thus solely determines the total number of particles:

$$C_p = \frac{\text{seed quantity in g/L}}{\rho_s\, l_p\, d_p^2} \quad (6.)$$

For a crystallisation with 100 g/L of solute seeded with 1 g/L of seed and using d_p=10 μm, l_p = 30 μm and ρ_p=1400 kg/m^3 gives an average centre-to-centre distance of $\delta_{p\text{-}p}$ = 160μm.

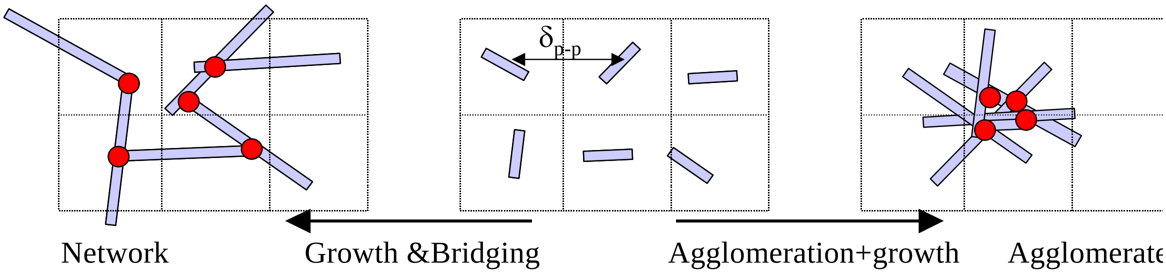

Figure 7: Structure formation from seed crystals
(i) Net work formation by particle growth + rotation (ii) agglomeration by translation

3.2 Describing "structure"

To form significant structure the particles need to interact. Two types of structures are possible (figure 7): (i) networks in which particles with $l_p/\delta_{p\text{-}p} > 1$ bridge the average distance between them and form junctions and (ii) agglomerates; particles converged into a single larger super particle. The average centre point distance of particles in this super particle $\delta_{p\text{-}p,agg}$ is thus smaller that $\delta_{p\text{-}p}$. Dense agglomerates are unlikely to generate a significant yield stress for as long as $\delta_{p\text{-}p,agg}/\delta_{p\text{-}p} << 1$ the average distance between the agglomerates is always larger than the average agglomerate size. Note this is not true if the agglomerates are one or two-dimensional structures (e.g. strings or sheets).

For crystallising systems it is more likely that networks are the cause of the rheological problems. Particles with lengths larger than $\delta_{p\text{-}p}$ can contact each other, and a "junction" can form between them. The strength of the junction (σ_j) depends on the nature of the bond and the cross sectional area of the junction. From the observations in the case study, it appears that junctions are formed during the main crystallisation, hence it is reasonable to assume that junctions are formed by bridges of crystallised solute.

The most likely contact between two needles randomly touching is a point contact between two of long ribs of the needle (figure 8a). If a small amount of material was deposited then the cross sectional area that needs to be broken determines the junction strength. It is assumed that the characteristic junction diameter d_j is much smaller then the particle diameter d_p; e.g. when force is exerted on the particles junctions will break well before the particle itself is broken.

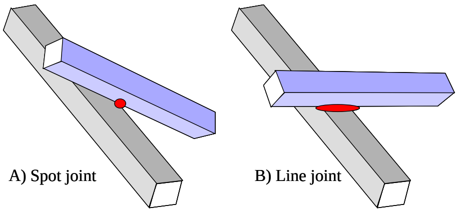

Figure 8: Junctions between two needles

The junction strength σ_j is determined by the amount of material deposited to form the junction and the stress required to break the solid (σ_s). Assuming the junction is formed as a sphere with diameter d_j, the number of moles in the junction (N_j) is described as:

$$\frac{dN_j}{dt} = k_l \, \pi \, d_j^2 \, \Delta C \qquad \text{and} \qquad \frac{d\,d_j}{dt} = \frac{2\,Mw}{\rho_s} k_l \, \Delta C \qquad (7.)$$

Assuming the growth is diffusion limited then Sherwood ($k_l \, d_j/D$) =2; integrating eq(7) gives:

$$d_j^2 = \frac{8\,D_{diff}\,Mw}{\rho_s} \int_0^{\tau_{form}} \Delta C \, dt \qquad (8.)$$

For a system with a $\Delta C = 10$ mg/ml (low) and a typical coefficient of molecular diffusion of 10^{-9} m^2/s this means that $d_j = 1$ μm for a formation time of just 0.02 s. The likely time for a junction to form is therefore treated as a constant independent of agitation in this work. The integral in equation (8) may then be replaced with a $\Delta C(t) \, \tau_{form}$.

The strength of a junction is proportional to the area formed on breaking the junction, and a shear stress σ^o which is a property of the solid:

$$\sigma_j \sim d_j^2 \sigma^o \sim \Delta C \sigma^o \qquad (9.)$$

The extent to which structure is formed can be described by the number concentration of junction in the fluid, C_j (number/m^3). the higher C_j the larger or stronger the structure formed. Note that the average number of junctions per particle $n_j = C_j/C_P$. The shear stress a structure can withstand is proportional to the number of junctions in a plane (number/m^2) which equals $C_j^{2/3}$. To generate movement in a plane these junctions need to be broken. The force/m^2 required to do this is the yield stress σ_y, which is equal to $C_j^{2/3}\ \sigma_j$:

$$\sigma_y \sim C_j^{2/3} \Delta C \sigma^o \qquad (10.)$$

3.3 The largest stable structure dimension

In an agitated system shear and turbulent forces on particles may cause junctions to break, and thus structure is reduced. By analogy with the largest stable drop size in dispersions, a largest stable structure size D_{st} can be defined: the junctions in that structure are just capable of withstanding the turbulence forces that act upon the structure:

$$\rho_C u'^2 \leq C_j^{2/3} \sigma_j \sim \sigma_y \qquad (11.)$$

The RMS velocity of the eddies that exert most force is proportional to $(\varepsilon\ D_{st})^{2/3}$ and the energy dissipation rate ε is proportional to N^3D^2 so the structure can not be broken up if:

$$\frac{\rho_C N^2 D^2}{\sigma_y}\left(\frac{D_{st}}{D}\right)^{2/3} \leq 1 \qquad \text{or} \qquad N_{Ni}\left(\frac{D_{st}}{D}\right)^{2/3} \leq 1 \qquad (12.)$$

Here we define the Nienow[1] number N_{Ni}: the ratio of the turbulent forces acting on the structure to its cohesive force. Note that for $N_{Ni} <= 1$ structure does not break up, and a cavern is formed the size of the agitator.

For the values of the yield stress observed in the case study (table 1) we can calculate the stable structure size inside the mobile zone by rearranging eq(12):

$$D_{st} = \frac{D}{N_{Ni}^{1.5}} \qquad (13.)$$

Table 1: structure size for the experiments in the case study

Caffeine (Mg/mL)	σ_y (Pa)	N (rpm)	N_{ni}	D_{st} (mm)
50	4	400	18	0.5
50	4	900	90	0.05
100	15	900	20	0.4
100	15	1200	35	0.2

From the table it is clear that no structure can remain in the mobile zone, as the primary particle length of ~1 mm (from microscopy) is significantly larger than D_{st}. When the agitation speed is increased to remobilise the system, the network is completely destroyed.

3.4 Qualitative predictions

Tixotropic fluids are of course well known examples of fluids with a rheology governed by formation and break up of structure. Møller et al (2006) give an excellent review of how these fluids can be modelled by modelling the dependence of the parameters in a rheological model ($\sigma = f(\gamma)$) on a structure parameter like the concentration of junctions C_j defined in this paper:

$$\sigma = \sigma_y(Cj) - \gamma\ \eta(Cj, \gamma) \qquad (14.)$$

$$\frac{\partial C_j}{\partial t} = f(C_j, \gamma) - g(C_j, \gamma) \qquad (15.)$$

Unfortunately, in a crystallising system the supersaturation ΔC plays an important role, and is not easy to assess or calculate. A simpler approach is based on the assumption that for a network to be able to withstand a force many particles need to have at least one junction, to allow them to “tangle” or two for particles to be fixed in the structure. It follows that Cj/Cp is in the order of 1. Note that Cj/Cp is ~1 only just after the system has become immobile at the

---

[1] Nienow and Elson (1988) first derived this number in their work on cavern formation in yield stress fluids. Note how this number simplifies equation (3); For $P_oN_{Ni} = 1$ the cavern size is similar to the agitator size, for $P_oN_{Ni} > 30$ the cavern can be assumed to have reached the vessel wall.

wall. For long particles and long periods of immobility yield stress is likely to increase as the number of junctions per particle and the strength of those junctions are likely to increase.

Just after system has set solid at the wall however the initial yield stress of a system can be estimated from eq(10) and using $C_j \sim C_p$:

$$\sigma_y \sim C_p^{2/3} \, \Delta C \, \sigma^o \sim X^{2/3} \, \Delta C \, \sigma^o \qquad (16.)$$

Here C_p is replaced with X, the total solute loading in mg/mL, as for a seed the crystallisation, the volume of seed particles, and thus C_p, are proportional to the solute loading.

The initial yield stress is therefore determined by the extent of ΔC and the solute loading X, NOT hydrodynamic forces. The manner in which super saturation is generated is thus extremely important. Differences in operation (antisolvent addition rate, cooling rate) may result in very different rheological behaviours.

In our work we found that values of $\sigma_y/X^{2/3}$ typically range between 0.1 and 0.8. This is based on a rather limited data set, that includes the data presented here, as well as unreported data for 2 other AstraZeneca processes. A "conservative" estimate of N_{Ni} would thus be:

$$N_{Ni} \approx \frac{\rho_C N^2 D^2}{\text{const } X^{2/3}} \qquad \text{const} \sim 1 \frac{\text{Pa}}{(\text{kg/m}^3)^{2/3}} \qquad (17.)$$

Based on this criterion, the appropriate agitation speed can be selected to match particular solid loading, as long as there is a degree of control of the supersaturation.

4 CONCLUSIONS

The formation of structure in crystallising systems can be successfully monitored using the Hydramotion RV900 viscosity probe; interestingly, it's measurement correlates to a system's yield stress. Modelling the structure formation let to the definition of the largest stable structure as a function of the Nienow number; the ratio of turbulent forces to the yield stress. The model also suggests that the Nienow number may be approximated using the solid loading. This has been successfully applied to avoid rheological problems in the lab by setting the solid concentration and agitation speed so that $N_{Ni}>50$. These systems should be scaled up to the plant using a constant Ni (=constant tip speed).

5 AKNOWLEDGEMENTS

The author likes to thank Lauren Wilkinson for the experimental work and Simon Black for his helpful comments and discussion.

6 REFERENCES

Borghesani A. F. (1985). Concentration-dependent behaviour of the shear viscosity of coal-fuel oil suspensions. Rheol Acta **24**, 189-197

Gay E.C., Nelson P.A., Armstrong W.P. (1969). AICHE J. **15**, 815.

Heymann L., Peukert S., Akse N. (2002). On the solid-liquid transition of concentrated Suspensions in transient shear flow. Rheol Acta **41**, 307–315

Møller P.C.F., Mewis J., Bonn D. (2006). Yieldstress and thixotropy: on the difficulty of measuring yield stresses in practice. Soft Matter **2**, 274–283

Nienow A.W.,Elson T.P. (1988). Aspects of mixing in rheologically complex fluids. Chem. Eng. Res. Des. **66,** 5-15.